Transverse coherence length of down-converted light in the two-photon state

E. J. S. Fonseca, C. H. Monken, and S. Pádua*

Departamento de Física, Universidade Federal de Minas Gerais, Caixa Postal 702, 30123-970 Belo Horizonte MG, Brazil

G. A. Barbosa

Departamento de Física, Universidade Federal de Alagoas, Cidade Universitária, 57072-970 Maceió Al, Brazil

(Received 9 June 1998)

Measurements of the Young interference pattern for down-converted light in the two-photon state are performed. Light in the two-photon state is generated at the output of a Hong-Ou-Mandel balanced interferometer. Two-photon interference patterns with visibilities up to 100% are obtained. Visibilities of the two-photon interference patterns as a function of the double-slit separation are obtained and show that the transverse coherence length of the two-photon light is much larger than the one-photon beam for the distances considered in the experiment. [S1050-2947(99)05702-9]

PACS number(s): 42.50.Ar

I. INTRODUCTION

Interference experiments with Young's double-slit and Michelson interferometers have had a very important role in the development of classical and quantum optics. Classical theory, based in the wave nature of light, has been able to explain the interference pattern for thermal-like sources and lasers [1]. Dirac, in his well known book [2], has given an explanation based on the quantum nature of light for these experiments. He argues that each photon interferes only with itself and the interference pattern results from the interference between the probability amplitudes of the two possible paths for the photon. The first experiment that tested this idea was already performed by Taylor in 1909 [3] by detecting a needle diffraction pattern with a very weak flame as light source such that on average only one photon at a time hits the needle. After a long time detection, the interference fringe pattern showed no difference from a high intensity pattern. Since this light source is chaotic [4], the assertion that only ''one photon'' hits the needle at a time is questionable. The first detected ''one-photon at a time'' interference pattern was obtained by Grangier, Roger, and Aspect by using a two-photon radiative atomic cascade as light source [5]. The Mach-Zehnder interference pattern of one of the photons was recorded in coincidence with the second emitted one in the cascade, not transmitted through the interferometer. This light source permits the detection of one photon state with probability close to 1.

Young's one-photon interference pattern has been recently studied for the case where the light source is a nonlinear crystal excited by a pump laser and emitting down-converted photons by the nonlinear optical process of the parametric luminescence [6–11]. In this process one photon of the pump laser with frequency ω_p and wave vector $\mathbf{k}_p$ is converted into two other ones, conventionally called signal (ω_s, $\mathbf{k}_s$) and idler (ω_i, $\mathbf{k}_i$). Energy ($\hbar\omega_p = \hbar\omega_s + \hbar\omega_i$) and

momentum ($\hbar\mathbf{k}_p = \hbar\mathbf{k}_s + \hbar\mathbf{k}_i$) of the photons are conserved. The spatial coherence properties of the down-converted beams were investigated by measuring the transverse coherence length of one of the beams [6] and studying experimentally and theoretically the nonlocal quantum correlations between them [7–11]. Young interference experiments with only one of the parametric down-converted beams shows that the measured fringes visibilities and the transversal coherence length are the expected ones for a classical extended thermal-like source [6].

In this paper we present experimental results of the Young's double-slit interference pattern of light in the two-photon state (two photons in the same wave packet). The aim of this work is to study the transverse fourth-order coherence of a light beam in this state. Experiments for the generation of light in two-photon wave packets were first performed by Hong, Ou, and Mandel (HOM) [12]. Twin parametric down-converted photons are combined in a 50/50% beam splitter and the number of coincident photons at the output of the beam-splitter are measured as a function of the optical path length difference of the photons. When this difference is approximately zero a null in the coincidence rate is detected. It has been shown that at this point the two photons always emerge together from either one of the beam-splitter exit ports [13,14]. By doing Young's interference experiments with the output light of the HOM interferometer, we are able to study the spatial coherence properties of the light in the two-photon state. The Young fringes visibilities and the measured transverse fourth-order coherence length are much larger than that obtained from the second-order Young's interference pattern with only one of the down-converted beams.

A simple theory can give us a clue of the expected Young's interference pattern when two photons hit at the same time a double slit [Fig. 1(a)]. As it will be clear below, our detector gives us the number of transmitted two-photon wave packets (*biphotons*) that arrive at a point P, with transverse position coordinate x. The probability amplitude associated with the possibility of one photon to be at the detector position x, after being transmitted through a double slit is

---

*Author to whom correspondence should be addressed. Electronic address: spadua@fisica.ufmg.br
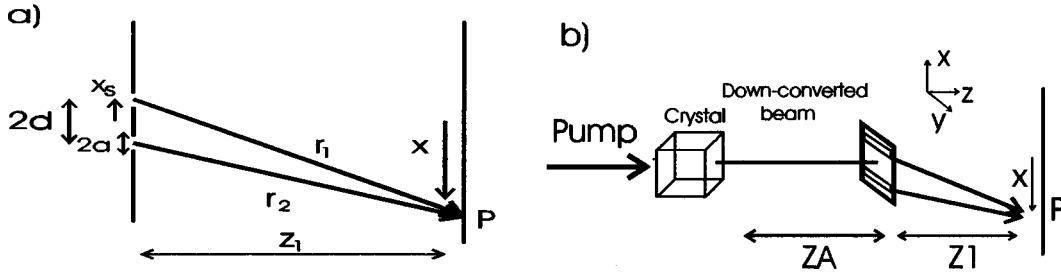
FIG. 1. (a) Schematic drawing of a Young double-slit experiment where $2a$ is the slit's width; $2d$ is the double-slit separation; z_1 is the distance between the double-slit and the detector planes; y,x are the transverse position coordinates; and r_1,r_2 are the distances between each slit and the detector positioned at point P. (b) Schematic drawing of a Young double-slit experiment where z_A is the distance between the crystal and the double-slit plane. Light is generated by a collinear parametric down-conversion process.

$$\Psi_1(x) \propto \int_{d-a}^{d+a} e^{ikr_1(x_s,x)} dx_s + \int_{d-a}^{d+a} e^{ikr_2(x_s,x)} dx_s, \quad (1)$$

where x_s,x are variable transverse coordinates; $k=2\pi/\lambda$ with λ being the wavelengths of the photons; $2d$ is the separation of the slits; $2a$ is the width of the slits. The distances between each slit and the point P at position x are

$$r_1(x_s,x) \approx z_1 + \frac{(x+x_s)^2}{2z_1}, \quad r_2(x_s,x) \approx z_1 + \frac{(x-x_s)^2}{2z_1}, \quad (2)$$

where z_1 is the distance between the double-slit plane and the observation screen [Fig. 1(a)]. Expression (1) is simplified further by doing a variable transformation $(x_s = x_s' + d)$ where it becomes clear that we can neglect $x_s'^2$ terms ($2d \gg a$) in $r_1(x_s',x)$ and $r_2(x_s',x)$. It becomes

$$\Psi_1(x) \propto e^{i\alpha(x)} [e^{i(kdx/z_1)} I_1 + e^{i(kdx/z_1)} I_2], \quad (3)$$

where $\alpha(x) = k(z_1 + [(x^2+d^2)/2z_1])$, $I_1(x) = 2a \, \text{sinc}\{[k(d+x)a]/z_1\}$ and $I_2(x) = 2a \, \text{sinc}\{[k(d-x)a]/z_1\}$. From expression (3) we obtain the probability amplitude associated with the arrival of two photons at position x at the same time: $\Psi_2(x) = \Psi_1(x)\Psi_1(x)$. Then the number of two photons that arrive at position x is proportional to

$$N_c(x) \propto \Psi_2^*(x)\Psi_2(x) = A(x) + 4B(x)$$
$$\times \cos\left(\frac{2kdx}{z_1}\right) + 2C(x)\cos\left(\frac{4kdx}{z_1}\right), \quad (4)$$

where $A(x) = I_1(x)^4 + I_2(x)^4 + 4I_1(x)^2 I_2(x)^2$; $B(x) = I_1(x)^3 I_2(x) + I_1(x)I_2(x)^3$ and $C(x) = I_1(x)^2 I_2(x)^2$. Expression (4) shows that the resultant interference pattern consists of two patterns, one of them with periodicity λ and the other one with periodicity $\lambda/2$. The diffraction terms in expression (4) are proportional to the fourth power of sinc functions. It is also easy to see that the visibility of the ''interference pattern'' is 1. This is expected because our simple theory does not include the light source size and the photons correlations. The light source is assumed to be a pointlike source. A more complete theory requires the calculation of the fourth-order correlation function by using a quantum multimode theory [14,15]. This theory [16,17] takes into account the spatial correlation of the down-converted photons.

It supposes that the two-photon wave packets are generated collinearly from the crystal. The number of two-photon packets hitting the detection screen, after being transmitted through a double slit, is proportional to the fourth-order correlation function calculated at position x,

$$N_c(x) \propto \langle \hat{E}_i^{(-)}(x)\hat{E}_s^{(-)}(x)\hat{E}_i^{(+)}(x)\hat{E}_s^{(+)}(x)\rangle, \quad (5)$$

where $\hat{E}_i^{(+)}(x)$ and $\hat{E}_s^{(+)}(x)$ are the idler and the signal transmitted electric field operators, respectively. The transmitted electric field operators are obtained by doing an analogy with the classical calculation of the electric field transmitted through an aperture when the angular spectrum of the field before the aperture (double slit) is known [14]. The electric field operator can be written as

$$\hat{E}_j^{(+)}(x) \propto e^{ikz} \int dq_j \int dq_j' \hat{a}(q_j') T(q_j - q_j')$$
$$\times e^{i[q_j x - q_j^2(z-z_A)/2k - q_j'^2 z_A/2k]}, \quad (6)$$

where $j=i$ (idler), s (signal); $k=k_s=k_i$ is the down-converted field wave vector magnitude; q_j, q_j' are x-transverse components of the wave vectors $\vec{k}$; $\hat{a}(q')$ is the annihilation operator associated with the mode q'; $T(u)$ is the Fourier transform of the double-slit aperture; z_A is the distance from the crystal to the double slit, x is the transverse position of the two-photon detector, and z is the longitudinal coordinate with origin at the crystal center [Fig. 1(b)].

Expression (5) is calculated by using the multimode two-photon wave function [18]. In the monochromatic ($\Delta\omega_j \ll \omega_j$, $j=s,i,p$), paraxial ($|q_j| \ll |k_j|$), and thin crystal approximation, the state generated by the parametric down-conversion process can be approximated by [17]

$$|\Psi\rangle = |\text{vac}\rangle + \text{const} \times \int dq_s \int dq_i v(q_s+q_i)|1,q_s\rangle|1,q_i\rangle, \quad (7)$$

where $v(q_s+q_i)$ is the angular spectrum of the pump beam. As it was shown recently [17], the angular spectrum of the pump laser beam is transferred to the fourth-order correlation of the down-converted two-photon pairs. After some algebra, we obtain the number of *biphotons* as a function of position x in the detection screen from expression (5) [Fig. 1(b)]:

$$N_c(x) \propto A(x) + 4B_1(x)B_2(x)\cos\left(\frac{kd^2}{z_A} + \frac{kx2d}{z_1}\right)$$

$$+ 4B_2(x)B_4(x)\cos\left(\frac{kd^2}{z_A} - \frac{kx2d}{z_1}\right)$$

$$+ 2B_1(x)B_4(x)\cos\left[\frac{2kx(2d)}{z_1}\right] \qquad (8)$$

with

$$A(x) = |B_1(x)|^2 + 4|B_2(x)|^2 + |B_4(x)|^2 \qquad (9)$$

$$B_1(x) = 4\sqrt{W(d,z_A)}a^2\,\mathrm{sinc}^2\left(\frac{k(x-d)a}{z_1}\right) \qquad (10)$$

$$B_2(x) = 4\sqrt{W(0,z_A)}a^2\,\mathrm{sinc}^2\left[\left(\frac{kx}{z_1} + \frac{kd}{L}\right)a\right]\mathrm{sinc}^2\left[\left(\frac{kd}{L} - \frac{kx}{z_1}\right)a\right], \qquad (11)$$

$$B_4(x) = 4\sqrt{W(-d,z_A)}a^2\,\mathrm{sinc}^2\left(\frac{k(x+d)a}{z_1}\right), \qquad (12)$$

where $2d$ is the separation of the double slit, $2a$ is the width of each slit, $L = z_1 z_A/(z_1 + z_A)$, and $W(x,z_A)$ is the spatial intensity distribution of the pump laser beam at the transverse position x and at the longitudinal distance z_A from the crystal. It is assumed that the double-slit plane is relatively far from the crystal and the detectors plane (''Fraunhofer regime''). By comparing expressions (4) and (8) we notice that the second and third terms in the right-hand side of expression (8) show the interference with periodicity of the down-converted photons and the fourth term represents an expected interference pattern from a light beam with wavelength $\lambda/2$. Note also that $B_1(x)$, $B_2(x)$, and $B_4(x)$ are proportional to the square root of the transverse intensity distribution of the pump laser at the position of the double slit. It is also worth mentioning that this fourth-order Young interference pattern depends on the spatial profile of the pump at the double-slit plane and not at the crystal position as in the Young second-order interference pattern [6].

Expression (8) can be further simplified by doing $B_1(x) \approx B_4(x)$,

$$N_c(x) \propto 2|B_1(x)|^2 + 4|B_2(x)|^2$$

$$+ 8B_1(x)B_2(x)\cos\left(\frac{kd^2}{z_A}\right)\cos\left(\frac{kx2d}{z_1}\right)$$

$$+ 2|B_1(x)|^2\cos\left[\frac{2kx(2d)}{z_1}\right]. \qquad (13)$$

For the range of experimental parameters used in these measurements, the third term on the right-hand side of expression (13) is much larger than the fourth term. Since the third term is dominant, we find the following expression for the visibility of the interference pattern:

$$V = \frac{2B_1(x)B_2(x)}{|B_1(x)|^2 + |B_2(x)|^2}\left|\cos\left(\frac{kd^2}{z_A}\right)\right|, \qquad (14)$$

where we have obtained the minimum in the pattern by making $kx2d/z_1$ equal to a multiple number of π, in expression (13). Notice that the third term on the right-hand side of expression (13) is not dominant on the fourth term when kd^2/z_A is close to a multiple number of $\pi/2$. For this case, the third term is much larger than the fourth one and the visibility of the resultant interference pattern is

$$V = \frac{|B_1(x)|^2}{|B_1(x)|^2 + 2|B_2(x)|^2}. \qquad (15)$$

Notice that for this range of parameters, the periodicity of the interference pattern becomes the one expected from a beam with the wavelength of the pump laser.

II. EXPERIMENTAL SETUP

A $20\,\mathrm{mm} \times 20\,\mathrm{mm} \times 20\,\mathrm{mm}$ $\mathrm{LiIO_3}$ crystal pumped by a 40-mW Kripton laser emitting at $\lambda = 413.1$ nm was used to generate type I down-conversion parametric luminescence. The measured Gaussian full width at half-maximum (FWHM) of the pump laser just before the crystal is 0.5 mm. Signal and idler beams with the same wavelength around 826 nm were selected by 2.0-mm-diam pinholes placed 100 mm from the crystal and making an angle of 34° with the pump laser beam. The down-converted beams were then combined in a 50/50% beam splitter BS1 for the generation of light in the two-photon state [12]. The arm lengths of the interferometer were balanced by displacing one of the 90° prisms shown in Fig. 2(a). This prism is mounted in a submicron translation stage. The optical length of each arm is approximately 570 mm. Down-converted beams are detected in coincidence at the output port of the 50/50% beam splitter. Light detectors are avalanche photodiodes, with resolution of 3 ns. The down-converted beams were focused on the detectors by means of microscope objective lenses. The two-photon interferometer was first aligned by using 0.9-nm-bandwidth Gaussian interference filters F, centered at 826.2 nm. Pulses from the detectors are sent to a photon counter and coincidence detection setup with 5 ns resolving time. The data are analyzed in a personal computer. Young double slits ($S2$) of different separations are placed in one of the exit paths of the interferometer [Fig. 2(b)]. The Young slits are made by a photographic process, producing a dark negative with two transparent slits. The width of each slit, $2a = 0.07$ mm and the distance between them, $2d = 0.16$, 0.25, 0.36, 0.45, 0.52, 0.60, 078 mm, were measured with a microscope. The double-slit plane (xy plane) is aligned perpendicular to the plane defined by the pump laser and the down-converted beams (yz plane) with the small dimension of the slits parallel to the x direction. They are placed 30 mm away from the BS1 beam splitter. The two-photon interference pattern is recorded by displacing a ''two-photon detector'' perpendicular to the plane defined by the pump and down-converted beams [19]. The ''two-photon detector'' consists of a single slit ($S1$) oriented parallel to the double slits, a 50/50% beam splitter BS2 and two avalanche photodiodes ($D3,D4$) detecting the photons in coincidence. We use a
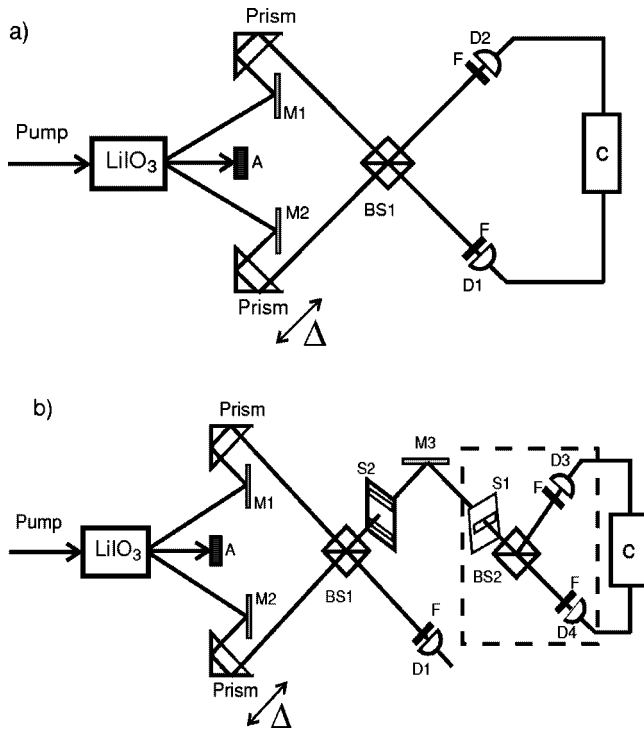
FIG. 2. (a) Outline of the experimental setup used to generate light in the two-photon state. BS1 is a beam splitter; $M1$ and $M2$ are mirrors; F is an interference filter; A is a beam stop; $D1$ and $D2$ are avalanche photodiode detectors; C is the coincidence detection system. (b) Outline of the experimental setup used to study the transverse coherence length of the two-photon light beam. The dashed square shows the two-photon detector. $M3$ is a mirror; $S2$ is a double slit; $S1$ is a single slit; $BS2$ is a beam splitter; F is a color glass cutoff filter; $D3$ and $D4$ are avalanche photodiode detectors; the distance between the planes of the single slit $S1$ and $S2$ is 410 mm except for the $2d=0.16$ mm double-slit measurement; optical path length of the down-converted photons from the crystal to $S2$ is 600 mm.

single slit of 0.3 mm width for recording the interference patterns of the $2d=0.25$, 0.36, 0.45, 0.52 mm double slits. The recording of the interference pattern of the $2d=0.16$, 0.60, 0.78 mm double slits was done with a 0.2 mm width single slit. The entire ''two-photon detector'' moves relatively to the Young double slits. The distance between the planes of the Young double slits and the two-photon detector slit is 230 mm for the $2d=0.16$ mm double slit and 410 mm for all the others. Besides these measurements, we took an extra one with the $2d=0.25$ mm Young double slits $S2$ and the single-slit $S1$ planes (xy planes) perpendicular to the plane (yz) defined by the pump laser and the down-converted beams with the small dimension of the slits parallel to the y direction.

III. RESULTS

Figure 3(a) shows the number of coincident counts between $D1$ and $D2$ as a function of the prism displacement Δ of the HOM interferometer [Fig. 2(a)]. A minimum in the number of coincidences, due to destructive interference at the beam splitter, is seen. With careful alignment we have been able to obtain coincidence dips up to 97%. The optical
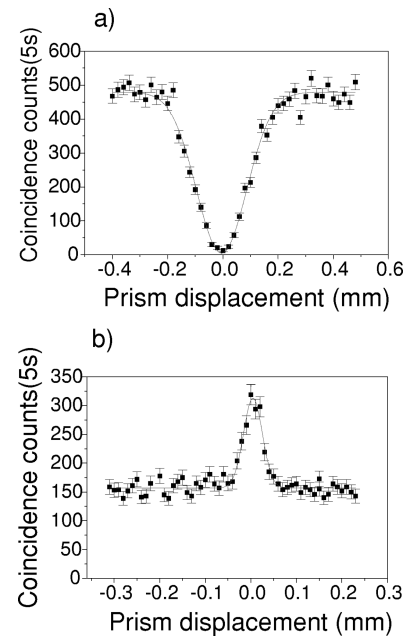

FIG. 3. (a) Coincidence counts between $D1$ and $D2$ detectors as a function of the prism displacement. (b) Coincidence counts between detectors $D3$ and $D4$ as a function of the prism displacement without the double slit. The continuous curves are Gaussian fittings.

path length from the crystal to detectors $D1$ and $D2$ was 1000 mm and their collection areas were defined by pinholes of 2.0 mm diameter placed in front of them. The 0.42-mm FWHM of the coincidence dip in Fig. 3(a) is a measurement of the coherence length for the photon wave packet seen by $D1$ and $D2$, and is determined by the 0.9-nm bandwidth of the interference filters. Once the minimum in the coincidence rate is found, the interferometer is set at this balanced point $\Delta \approx 0$. At this point, approximately 97% of the down-converted photons, pairs leave either one of the output ports of BS1 as two-photon wave packets (*biphotons*). In order to increase the detection efficiency, the narrow-band interference filters were replaced by color glass filters. A consequent narrowing of the coincidence dip width was observed, indicating the expected decrease of the photon coherence length, with no harm to the contrast of approximately 97%. The stability of the HOM interferometer was systematically checked during the experiment, and deviations of less than 3% in the coincidence dip were observed. Figure 3(b) shows the number of coincidences registered by the ''two-photon detector'' $D3-D4$ as a function of Δ, when the double slit is not in place. The visibility of the coincidence peak is close to the theoretically predicted maximum of 50%.

Second- and fourth-order interference patterns are shown in Fig. 4 for double-slit separation of 0.36 mm (a,b), 0.60 mm (c,d), and 0.25 mm (e,f). The measurements shown in Figs. 4(e) and 4(f) were taken with the slits perpendicular to the plane defined by the pump and the down-converted beams. The fourth-order interference pattern is obtained from the coincidence counts between $D3$ and $D4$ as a function of the ''two-photon detector'' transverse position, while the second-order pattern is obtained from the single counts. Both patterns are recorded at the same time. The second-order pattern was fit to the function
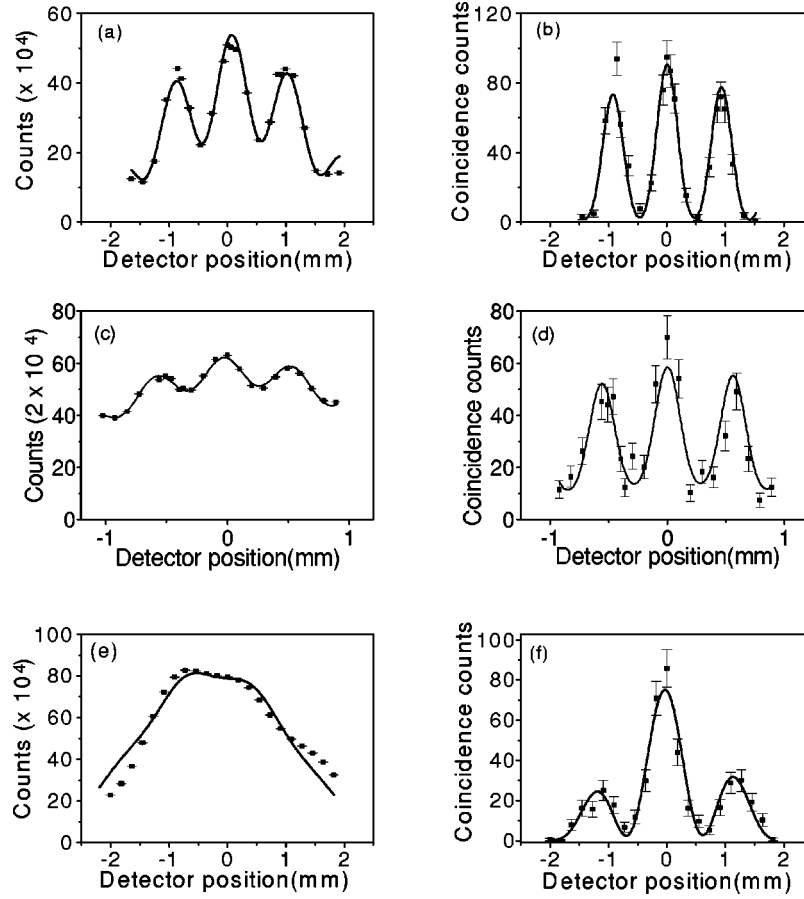
FIG. 4. Second-order [(a), (c), and (e)] and fourth-order [(b), (d), and (f)] Young interferograms and fittings, for double slits with separations $2d = 0.36$ mm (a) and (b), 0.60 mm (c) and (d), and $2d = 0.25$ mm. The double-slit plane (xy plane) was perpendicular to the pump–down-converted beams plane (yz plane). For the measurements shown in (a)–(d), the small dimension of the slits is in the x direction. For (e) and (f) the slits were rotated by 90° having their small dimension in the y direction. Singles and coincidence counts detection times were 1000 s for (a), (b), (e), and (f), and 2000 s for (c) and (d) interferograms.

$$N(x_o) = \frac{N_o}{b} \int_{x_o - b/2}^{x_o + b/2} [\operatorname{sinc}(Ex)]^2 [1 + V_2 \cos(Fx + \beta)] dx, \tag{16}$$

where N_o is a normalization constant, $E = ka/z_1$, k is the wave number of the down-converted light beams, z_1 is the distance between the planes of the double slit and the "two-photon detector" entrance slit and $F = k2d/z_1$. The finite size of the detector was taken into account by integrating the intensity distribution between $x_o - (b/2)$ and $x_o + (b/2)$, where b is the width of the single slit $S1$ of the two-photon detector and x_o is the two-photon detector transverse position. The adjusted parameters were the visibility V_2, the phase offset β, and the constant N_o. Similarly, the fourth-order pattern was fit to the function

$$N_c(x_o) = \frac{N_1}{b} \int_{x_o - (b/2)}^{x_o + (b/2)} [2|B_1(x)|^2 + 4|B_2(x)|^2$$
$$+ 4V_4 [|B_1(x)|^2 + |B_2(x)|^2] \cos(Fx)$$
$$+ 2|B_1(x)|^2 \cos(2Fx)] dx, \tag{17}$$

where parameters were the normalization constant N_1, the

visibility V_4. This expression is obtained by substituting Eq. (14) in Eq. (13) and calling V the experimental parameter V_4.

Figure 5 shows the visibilities V_2—expression (16)—and V_4—expression (17)—of the second- and fourth-order interference patterns, respectively, as functions of the double-slit separation $2d$. These visibilities were obtained from the best
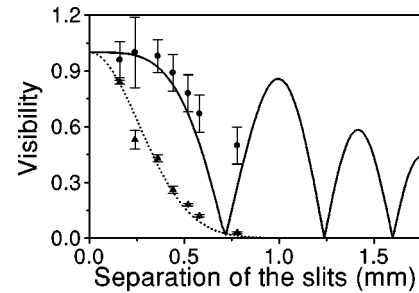

FIG. 5. Experimental points showing the visibility of the second-order (triangle) and fourth-order (squares) Young interferograms as a function of the double-slit half-separation. The dot curve is a Gaussian fit with HWHM of 0.32 ± 0.02 mm for the second-order data. The continuous curve is the predicted theoretical visibility obtained from expression (14), for the fourth-order interference pattern.

fits of the experimental data, taking into account the statistical error bars in each data point.

IV. DISCUSSION

The two-photon detector collects only those photon pairs that fall in the same spatial region defined by its entrance slit $S1$. A similar detection scheme was used for the time-resolved two-photon interference detection in a Michelson interferometer [19]. Fourth-order interference patterns, which we identify as the biphoton interference pattern, with visibilities near or larger than 90% were obtained in four of the seven measured interference patterns, with the double slit parallel to the pump–down-converted beams plane. These values are much higher than the measured second-order visibilities [6], which are known to be the same as in a photon-by-photon experiment as discussed in the Introduction. The periodicity of all the one- and two-photon measured interference patterns is the same and that is obtained from the wavelength of the down-converted photons, $\lambda = 826.2$ nm. This was checked by repeating the same experiment in the same geometrical conditions with a laser operating at $\lambda = 826.2$ nm. Although the fourth-order interference pattern has a component with periodicity $\lambda/2$ [see expression (4)], its contribution is very small as discussed before. A fourth-order Young interference pattern with 100% visibility was also measured with the small dimension of the double slit parallel to the pump–down-converted beams plane. For this case [Figs. 4(e) and 4(f)] practically no second-order interference [Fig. 4(e)] is observed and a pure two-photon effect is detected. The one-photon transverse coherence length parallel to the pump–down-converted beams plane is much smaller than the transverse coherence length in the direction perpendicular to this plane, at the same distance from the crystal (light source). This is consequence of the fact that the ''effective'' size of the light source in the direction parallel to the pump–down-converted beams plane is much larger than in the orthogonal direction [6].

Figure 5 compares the second- and fourth-order transverse coherence length of the down-converted light two-photon light by plotting the visibilities of the second- and fourth-order interference patterns as functions of the double-slit separation, with the double slit aligned to the pump–down-converted beams plane. We fit the second-order interference data with a Gaussian function having the Gaussian widths as an adjustable parameter. We use the obtained half-width at half-maximum (HWHM) of the Gaussian curve as our definition of the transverse coherence length (l_c). We clearly see that the transverse coherence length of the biphoton field is larger than the one-photon coherence length. For double slits with separation 0.60 and 0.78 mm we see practically only two-photon state light interference with visibility $60 \pm 8\%$ and $50 \pm 10\%$, respectively. This is the spatial analog to the Michelson and Mach-Zehnder interference pattern measurements of light in the two-photon state [19,20]. In those measurements the authors detect a two-photon interference pattern for optical path difference much larger than the one-photon longitudinal coherence length. Rarity et al. [20] affirmed that the interference oscillations are expected to disappear when the path-length difference in the Mach-Zehnder interferometer exceeds the longitudinal coherence length of the pump beam. If we establish an analogy to the spatial coherence case we expect that the biphoton beam to be transversally coherent like the pump beam. In fact, the data of Fig. 5 shows biphoton interference patterns with visibilities near 100% (within the error bar) in four of the seven measured double slits, as expected from a coherent beam. On the other hand, we detected fourth-order interference pattern with visibilities smaller than 90% for slits separation larger than 0.5 mm, suggesting that the transverse coherence length of the biphoton beam is smaller than the pump beam transverse coherence length. Therefore, the transverse coherence properties of the biphoton beam are totally different from the one-photon beam. Figure 5 also shows a continuous line that is obtained from the theoretical expression for the visibility. For the range of experimental parameters measured, the expression (14) gives the expected behavior for the fourth-order interference pattern visibilities as a function of the separation between the slits. We see a good agreement between the measured points and the theoretical predicted results. For this comparison we have measured the transverse intensity profile of the laser beam $W(x, z_A)$ at the distance $z_A = 600$ mm ''after'' the crystal plane. The measured profile is fitted to a Gaussian intensity distribution and this expression is used for calculating the theoretical formula of the visibility expression (14). We also notice an oscillation of the interference pattern visibility as the separation of the slits increases. More experimental visibility data points are necessary to check this behavior.

V. CONCLUSIONS

Young's interference fringe pattern for light in the two-photon state was experimentally investigated. A two-photon light beam is generated by a balanced Hong-Ou-Mandel type interferometer. The two-photon Young's pattern is obtained by measuring the number of transmitted biphotons through the double slit as a function of the two-photon detector position. This interference pattern shows much higher visibility than the ordinary second-order interference pattern. Biphoton interference patterns with $100 \pm 10\%$ visibility have been measured. By doing the same measurements for double slits with different separations and plotting the visibility of the interference patterns as a function of the slit separations we observed that the transverse fourth-order coherence length of the light beam in the two-photon state in our setup is much larger than the transverse second-order coherence length. A quantum multimode theoretical calculation gives results that are in agreement with the experimental data. The theoretical expressions show that the visibility of the fourth-order interference pattern depends on the distance between the crystal and the double-slit plane, the slit separation, and the transverse electric field profile at the position of the double slits.

[1] M. Born and E. Wolf, *Principles of Optics* (Pergamon Press, Oxford, 1993).

[2] P. A. M. Dirac, *The Principles of Quantum Mechanics* (Clarendon Press, Oxford, 1947).

[3] G. I. Taylor, Proc. Cambridge Philos. Soc. **15**, 114 (1909).

[4] D. F. Walls and G. J. Milburn, *Quantum Optics* (Springer-Verlag, Berlin, 1994).

[5] P. Grangier, G. Roger, and A. Aspect, Europhys. Lett. **1**, 173 (1986).

[6] P. H. S. Ribeiro, C. H. Monken, and G. A. Barbosa, Appl. Opt. **33**, 352 (1993).

[7] P. H. S. Ribeiro, S. Pádua, J. C. Machado Silva, and G. A. Barbosa, Phys. Rev. A **49**, 4176 (1994).

[8] D. V. Strekalov, A. V. Sergienko, D. N. Klyshko, and Y. H. Shih, Phys. Rev. Lett. **74**, 3600 (1995).

[9] P. H. S. Ribeiro and G. A. Barbosa, Phys. Rev. A **54**, 3489 (1996).

[10] J. Rehacek and J. Perina, Opt. Commun. **125**, 82 (1996).

[11] G. A. Barbosa, Phys. Rev. A **54**, 4473 (1996).

[12] C. K. Hong, Z. Ou, and L. Mandel, Phys. Rev. Lett. **59**, 2044 (1987).

[13] Z. Ou, C. K. Hong, and L. Mandel, Opt. Commun. **63**, 118 (1987).

[14] L. Mandel and E. Wolf, *Optical Coherence and Quantum Optics* (Cambridge University Press, Cambridge, 1995).

[15] L. J. Wang, X. Y. Zou, and L. Mandel, Phys. Rev. A **44**, 4614 (1991).

[16] C. H. Monken, E. J. S. Fonseca, and S. Pádua (unpublished).

[17] C. H. Monken, P. H. S. Ribeiro, and S. Pádua, Phys. Rev. A **57**, 3123 (1998).

[18] Z. Y. Ou, L. J. Wang, and L. Mandel, Phys. Rev. A **40**, 1428 (1989).

[19] J. Brendel, E. Mohler, and W. Martienssen, Phys. Rev. Lett. **66**, 1142 (1991); J. Brendel, W. Dultz, and W. Martienssen, Phys. Rev. A **52**, 2551 (1995).

[20] J. Rarity, P. R. Tapster, E. Jakeman, T. Larchuk, R. A. Campos, M. C. Teich, and B. E. A. Saleh, Phys. Rev. Lett. **65**, 1348 (1990).